

Saddle-point excitons in solids and superlattices

Hanyou Chu and Yia-Chung Chang

Department of Physics and Materials Research Laboratories, University of Illinois at Urbana-Champaign, Urbana, Illinois 61801

(Received 13 April 1987; revised manuscript received 26 May 1987)

A new method has been developed to study saddle-point excitons in solids and semiconductor superlattices. Interband absorption spectra of solids within simple tight-binding models are calculated with the inclusion of the electron-hole Coulomb interaction. Absorption spectra associated with saddle-point exciton resonances in superlattices are also studied as functions of the layer thickness.

In the past, excitonic effects associated with singularities in the density of states of solids have attracted a great deal of interest both theoretically and experimentally.¹⁻⁷ One of these singularities is associated with the M_1 saddle point in the band structure. Several authors have previously studied the absorption spectra of systems with such a singularity by approximating the electron-hole Coulomb interaction with a contact potential.^{2,3} The adiabatic approximation has also been used to study the saddle-point excitons with Coulomb interactions.⁴ In superlattices, the zone-folding effect of the band structure can lead to a series of M_1 saddle points at the minizone boundary. The Coulomb interaction between electrons and holes associated with these saddle-point states gives rise to exciton resonances below the energy of the saddle point. Semiconductor superlattices are ideal materials for studying the structure of saddle-point excitons because the band parameters near the saddle point can be tailored by varying the layer thicknesses and band gaps of the constituent materials. Experimental techniques (photoabsorption, excitation spectroscopy, and resonant Raman scattering) for probing the line shapes of saddle-point exciton resonances in superlattices are readily available. With the aid of modern computers, we have performed quantitative calculations for the line shapes of photoabsorption (or excitation) spectra associated with saddle-point excitons in a two-dimensional (2D) and a three-dimensional (3D) tight-binding model for bulk materials and in a Kronig-Penney model for semiconductor superlattices. We have compared our results for the tight-binding model systems with those obtained by using a contact potential.^{2,3} We find that the results calculated with the contact potential agree qualitatively with our results if a proper strength of the contact potential is chosen. For superlattices, we calculate the change of line shapes of the absorption spectra from three-dimensional-like in the ultra thin barrier case to two-dimensional-like in the wide-barrier case.

We shall consider the absorption coefficient of a solid including the electron-hole Coulomb interaction. The absorption coefficient for interband transitions can be written as

$$\alpha(E) = \sum_i |\Phi_i(0)|^2 \delta(E_i - E),$$

where $\Phi_i(\mathbf{r})$ is the wave function of the i th excitonic

states with an energy eigenvalue E_i . Here the label i runs through discrete states as well as the continuum states. The Schrödinger equation for an excitonic state Φ can be written in \mathbf{k} space as

$$\int d\mathbf{k}' \langle \mathbf{k} | H | \mathbf{k}' \rangle \phi(\mathbf{k}') - E\phi(\mathbf{k}) = 0, \tag{1}$$

where $\Phi = \int d\mathbf{k} \phi(\mathbf{k}) | \mathbf{k} \rangle$ and $| \mathbf{k} \rangle$ denotes the electron-hole product state at \mathbf{k} with the orthonormal condition $\langle \mathbf{k} | \mathbf{k}' \rangle = \delta(\mathbf{k} - \mathbf{k}')$. The wave vector \mathbf{k} is confined to the first Brillouin zone of the crystal system. The Hamiltonian H in \mathbf{k} space is given by

$$\langle \mathbf{k} | H | \mathbf{k}' \rangle = E_{cv}(\mathbf{k}) \delta(\mathbf{k} - \mathbf{k}') + \langle \mathbf{k} | v | \mathbf{k}' \rangle, \tag{2}$$

where $E_{cv}(\mathbf{k})$ is the energy difference between the conduction- and valence-band states at \mathbf{k} and v denotes the electron-hole Coulomb interaction. Neglecting umklapp terms,⁸ we can approximate the Coulomb matrix elements by

$$\langle \mathbf{k} | v | \mathbf{k}' \rangle = \begin{cases} \frac{e^2}{2\pi^2 \epsilon |\mathbf{k} - \mathbf{k}'|^2} & \text{for a 3D system,} \\ \frac{e^2}{2\pi \epsilon |\mathbf{k} - \mathbf{k}'|} & \text{for a 2D system,} \end{cases}$$

where ϵ is the static dielectric constant of the solid. For a superlattice, we write $\mathbf{k} = (\mathbf{k}_\parallel, q)$, where \mathbf{k}_\parallel is the projection of \mathbf{k} in the plane normal to the growth direction and q is the projection of \mathbf{k} in the growth direction. The Coulomb matrix element for superlattice states is given by⁹

$$v(\mathbf{k}, \mathbf{k}') = \frac{e^2}{2\pi^2 \epsilon} \sum_l F_e(q, q' - lK) F_h(q, q' - lK) \times \frac{1}{|\mathbf{k}_\parallel - \mathbf{k}'_\parallel|^2 + (q - q' + lK)^2}, \tag{3}$$

where

$$F_e(q, q') = \sum_n f(q + nK) f(q' + nK)$$

and $f(q + nK)$ is the projection of the superlattice wave function $\psi_q(z)$ for the electron in the plane-wave basis $e^{i(q+nK)z}$. $K = \pi/d$, where d is the length of the superlattice unit cell. $F_h(q, q')$ is similarly defined for the hole. In the same spirit we shall make the following approxima-

tion:

$$\Phi(0) = \int d\mathbf{k} \phi(\mathbf{k}) \langle 0 | \mathbf{k} \rangle \approx \int d\mathbf{k} \phi(\mathbf{k}) .$$

To solve the integral equation (1), we divide the first Brillouin zone into small equally sized subregions with volume (or area) Δ , each centered at a point denoted \mathbf{k}_j . We then replace the integral over the continuous variable \mathbf{k} by a summation over the discrete mesh points \mathbf{k}_j . Equation (1) is then converted into a matrix equation

$$[E_{cv}(\mathbf{k}_j) - E] \psi(\mathbf{k}_j) + \sum_{j'} \langle \mathbf{k}_j | v | \mathbf{k}_{j'} \rangle \psi(\mathbf{k}_{j'}) = 0 , \quad (4)$$

where $\psi(\mathbf{k}_j) = \phi(\mathbf{k}_j) \sqrt{\Delta}$. However, the above method would encounter a difficulty when the potential v has singularities in \mathbf{k} space, as it does in the present case. To circumvent this we integrate the potential function over each small subregion, while ignoring the weak \mathbf{k} dependence of the wave function $\phi(\mathbf{k})$ in that subregion. This will eliminate the singularities and we finally arrive at a simple eigenvalue problem:

$$\sum_{j'} \bar{H}_{j,j'} \psi(\mathbf{k}_{j'}) - E \psi(\mathbf{k}_j) = 0 , \quad (5)$$

with

$$\bar{H}_{j,j'} = \frac{\int_{\Delta_j} d\mathbf{k} \int_{\Delta_{j'}} d\mathbf{k}' H(\mathbf{k}, \mathbf{k}')}{\Delta} , \quad (6)$$

where Δ_j denotes a volume (area) centered at \mathbf{k}_j . After some mathematical manipulations, the multidimensional integral in Eq. (6) can be reduced to a one-dimensional integral involving special functions, which is then performed by numerical methods.⁹ Equation (5) can then be diagonalized to give the energies and corresponding wave functions for a few low-lying discrete exciton states and a good sampling of the continuum states.

We can derive Eq. (5) from a different point of view which adds some insight into our approach. Consider a set of basis states defined by $\beta_j = \int_{\Delta_j} d\mathbf{k} |\mathbf{k}\rangle / \sqrt{\Delta}$. Expand the excitonic state Φ in terms of the basis states β_j , i.e., $\Phi = \sum_j \psi(\mathbf{k}_j) \beta_j$ and then substitute the expansion into the Schrödinger equation for Φ , we again obtain Eq. (5). Thus the method can also be viewed as a variational method for obtaining the low-lying discrete exciton states. In addition, because the basis set chosen is a good sampling of all continuum states, we also obtain information about the perturbation of the continuum due to the electron-hole Coulomb interaction.

To minimize the size of the matrix to be diagonalized, while maintaining high precision, we shall fully exploit the symmetry of the system. Note that the absorption spec-

trum only depends on $\Phi(0)$, which is nonzero only for states with the full symmetry of the system (namely, s -like states for a system with rotational invariance, or A_1 -symmetry states for a system invariant under some point operations). Thus, for a cubic system, we can divide the first Brillouin zone into 48 equivalent segments. We define symmetrized basis states as $\bar{\beta}_j = \sum_R \beta_{Rj}/48$, where R runs over the 48 point operations of the group O_h , j runs over mesh points \mathbf{k}_j in a given segment, and β_{Rj} is β_j transformed by a point operation R . If $(2n)^3$ mesh points in the entire Brillouin zone are to be used, then the symmetrization procedure reduces the number of basis states to $n(n+1)(n+2)/6$ (almost a factor of 48). Similarly, for a 2D system with square symmetry, we can reduce the number of basis states from $(2n)^2$ to $n(n+1)/2$. In our calculations, we have used $n=16$ and 40 for the 3D and 2D models, respectively. We have tested the numerical results by using $n=10, 12$, and 15 for the 3D model and found that the results are insensitive to n when $n \geq 12$, indicating that convergence is achieved. For the 2D model, we found that it converges when $n > 15$.

For superlattices, we are interested in states with q in the entire minizone and with \mathbf{k}_\parallel near the zone center. We approximate the band structure in the parallel direction by a parabolic expression. Thus the system has a circular symmetry in parallel directions and a reflection symmetry in the growth direction. Symmetrized basis states are labeled by the radial component of \mathbf{k}_\parallel and q . A cut-off Λ is introduced for the sampling of k_\parallel . The final results for energies near the saddle point are insensitive to the choice of the cutoff, as long as Λ is large enough (about $20E_X$, where E_X is the bulk exciton binding energy).

In order to obtain a smooth absorption spectrum, we replace the δ function in Eq. (1) by a Lorentzian function with a half-width at half maximum Γ , viz.,

$$\delta(E_i - E) \approx \Gamma / \pi [(E_i - E)^2 + \Gamma^2] .$$

The magnitude of Γ is roughly equal to the energy spacing of the eigenstates. To examine the level of accuracy of the present method, we have calculated the absorption spectra for ideal 3D and 2D exciton systems (with parabolic bands) using the method described above. The results are found in excellent agreement with the analytical results which are already available for these systems.^{10,11}

We have used the \mathbf{k} -space sampling method to calculate the absorption spectra in a tight-binding model for a 3D system with cubic symmetry and a 2D system with square symmetry. We assume that the energy difference between the conduction band and valence band at wave vector \mathbf{k} can be written in the following tight-binding form:

$$E_{cv}(\mathbf{k}) = \begin{cases} E_0[3 - \cos(k_x a) - \cos(k_y a) - \cos(k_z a)] & \text{for a 3D system,} \\ E_0[2 - \cos(k_x a) - \cos(k_y a)] & \text{for a 2D system,} \end{cases}$$

where E_0 is a measure of the bandwidth and a is the lattice constant. A Bravais lattice is assumed; however, the extension of the present theory to lattices with a basis is straightforward. Figures 1 and 2 show the calculated absorption spectra for the 2D and 3D model systems, respectively, for various values of $\sigma = e^2/\epsilon a E_0$, which is the ratio

of the Coulomb interaction strength ($e^2/\epsilon a$) to the band parameter (E_0). For comparison, we have also plotted the analytical (dashed) and numerical results (dotted) for the system with no Coulomb interaction. In the 2D system, the density of states has a logarithmic singularity at the center of the band. Because of the broadening introduced

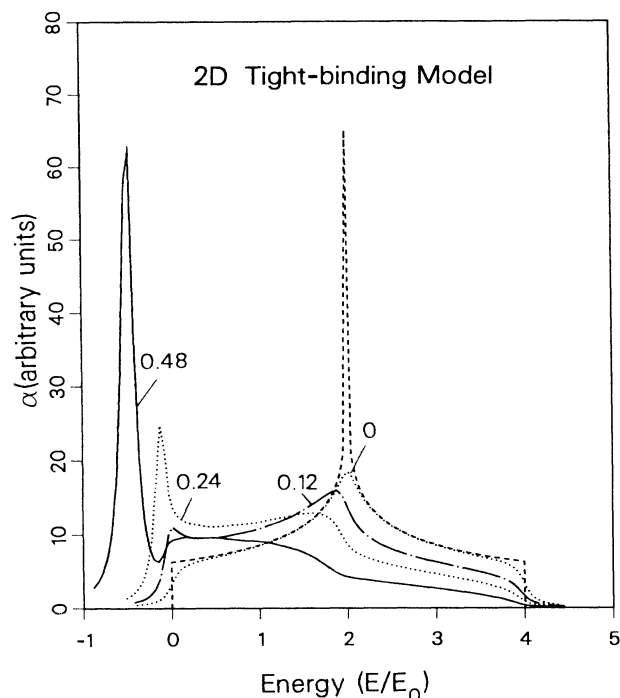


FIG. 1. Absorption coefficient of a 2D tight-binding model for various strengths of the Coulomb interaction ($\sigma=0, 0.12, 0.24, \text{ and } 0.48$).

in the numerical method, this singular structure becomes a broad peak. We can see from Figs. 1 and 2 that except near the singular points the numerical results agree with the analytical results very well. For realistic experimental data the broadening is always present due to the finite lifetime of the excitonic states and the resolution of the apparatus. Because of the sum rule, the total integrated area of the absorption curve is the same for any interaction strength. As the interaction becomes stronger (compared to the bandwidth), more states are pulled down to lower energies. For the 2D system, the saddle point with a logarithmic singularity is located at the center of the band. The peak structure is shifted to the lower-energy side when the Coulomb interaction is turned on, which is interpreted as a saddle-point exciton resonance. In addition, a bound-state peak appears below the lower edge of the band (onset of the band-to-band transition) due to the Coulomb interaction. The bound-state peak becomes more and more prominent and the resonance peak becomes weaker and weaker as the strength of the Coulomb interaction increases. As the interaction further increases (e.g., $\sigma=0.48$), a shoulder appears at the lower edge of the band while the peak corresponding to the saddle-point exciton disappears, resulting in a gradual falling off of α . It is not clear whether the shoulder near the lower edge of the band is associated with the excited bound states or with a pure resonance due to the nature of the numerical method. For the 3D systems, the interaction has to be strong enough for the system to have a bound state. A

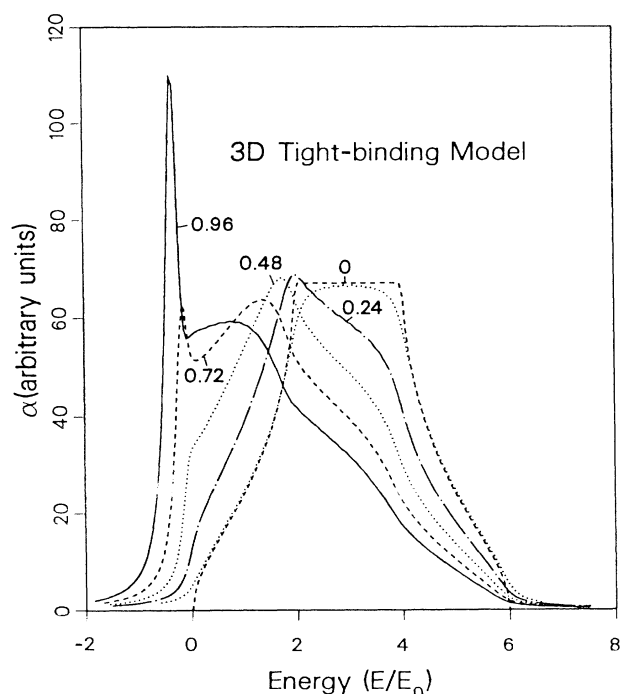


FIG. 2. Absorption coefficient of a 3D tight-binding model for various strengths of the Coulomb interaction ($\sigma=0, 0.24, 0.48, 0.72, \text{ and } 0.96$).

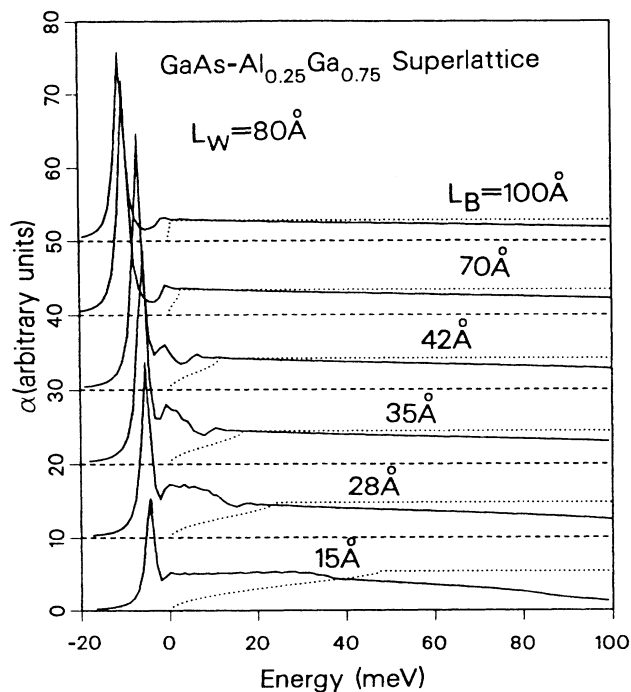


FIG. 3. Absorption coefficient of a series of GaAs- $\text{Al}_{0.25}\text{Ga}_{0.75}$ superlattices with GaAs width $L_w=80 \text{ \AA}$ and $\text{Al}_{0.25}\text{Ga}_{0.75}$ widths $L_B=15, 28, 35, 42, 70, \text{ and } 100 \text{ \AA}$.

bump appears below the first saddle point which can be identified as saddle-point exciton resonance. The results here bear some remarkable resemblance to the results obtained by using a contact-potential interaction.³ However, in Ref. 3, the peak structure near the band edge is due to the resonance effect, whereas the similar structure obtained in our calculation is due to the bound state of the exciton. Furthermore, in the 2D model, the contact potential calculation predicts a vanishing α at the center of the band and our calculation shows no such behavior.

We have also calculated the absorption spectra for GaAs-Al_xGa_{1-x}As superlattices in which M_1 saddle points exist at the minizone boundary whenever the energy dispersion as a function of q is a maximum there. Figure 3 shows the absorption spectra associated with the saddle-point exciton in GaAs-Al_{0.25}Ga_{0.75}As superlattices for a number of Al_{0.25}Ga_{0.75}As layer thickness (L_B). The width of the GaAs layer (L_W) is kept at 80 Å. All spectra are broadened by a Lorentzian function with a width of 1.2 meV. The dashed curves are the absorption spectra in the absence of the electron-hole Coulomb interaction. Because of the finite number (around 800) of basis states used in our calculations, the absorption coefficient tends to drop below that of the noninteracting case (dashed curve) as the photon energy goes above the saddle point. If an infinite number of basis states were used, the absorption coefficient for energies above the saddle point should decrease slowly, but remain slightly higher than the noninteracting value for all finite energies.¹² This discrepancy is present only at the high-energy side of all curves shown in this figure. For the thickest-barrier case ($L_B = 100$ Å) the band structure is dispersionless in the growth direction and our resulting absorption spectrum is similar to that of a quantum well (a quasi-two-dimensional system) at the

low-energy side. For the thinnest-barrier case ($L_B = 15$ Å) the dispersion in the growth direction is large and our resulting absorption spectrum for energies below the saddle point is similar to that of bulk GaAs. For energies near the saddle point the absorption coefficient dips down and smoothly joins a curve appropriate for a two-dimensional system. In the intermediate regime ($L_B = 28-70$ Å), we find prominent structures between the main exciton peak and the saddle point, indicating a redistribution of the oscillator strengths of the continuum states by the Coulomb interaction. These structures may be interpreted as exciton resonances. High-resolution excitation spectroscopy measurements for a large number of GaAs-Al_xGa_{1-x}As superlattices (including part of the series of samples adopted in Fig. 3) have recently been performed.¹³ Variation of the line shape of the absorption spectra due to the change of barrier thickness is apparent. We find qualitative agreement between our theoretical predictions and the experimental data. However, because of the difficulty in preparing precise superlattice structure, the inhomogeneous broadening tends to smear out the structures associated with the saddle-point excitons. Detailed comparisons between the theory and experiment will be reported elsewhere.

The authors have benefited from fruitful discussions with J. J. Song, J. N. Schulman, and M. V. Klein. This work was supported in part by the University of Illinois Materials Research Laboratory under the National Science Foundation (NSF) Contract No. NSF-DMR-83-16981. The use of the computing facilities of the National Center for Supercomputing Applications (NCSA) under the NSF grant is gratefully acknowledged.

¹J. C. Phillips, Phys. Rev. **136**, A1705 (1964).

²B. Velicky and J. Sak, Phys. Status Solidi **16**, 147 (1966).

³H. Kamimura and K. Nakao, J. Phys. Soc. Jpn. **24**, 1313 (1968).

⁴E. O. Kane, Phys. Rev. **180**, 852 (1969).

⁵J. E. Rowe, F. H. Pollak, and M. Cardona, Phys. Rev. Lett. **22**, 933 (1969).

⁶S. Antoci, E. Reguzzoni, and G. Samoggia, Phys. Rev. Lett. **24**, 1304 (1970).

⁷I. Balslev, Solid State Commun. **52**, 351 (1984).

⁸W. Kohn and J. M. Luttinger, Phys. Rev. **98**, 915 (1955).

⁹H. Y. Chu and Y. C. Chang (unpublished).

¹⁰M. Shinada and S. Sugano, J. Phys. Soc. Jpn. **21**, 1936 (1966).

¹¹See, for example, F. Bassani and C. P. Parravicini, *Electronic States and Optical Properties in Solids* (Pergamon, New York, 1975).

¹²G. D. Sanders and Y. C. Chang, Phys. Rev. B **35**, 1300 (1987).

¹³J. J. Song (private communication).